Raman spectroscopy as a tool to investigate structure and electronic properties of carbon atomic wires

Alberto Milani[1,2], Matteo Tommasini[1,2], Valeria Russo [2,3], Andrea Li Bassi[2,3], Andrea Lucotti[1,2], Franco Cataldo[4,5], Carlo S. Casari[2,3,*]

[1] Department of Chemistry, Materials and Chemical Engineering 'G. Natta', Politecnico di Milano, piazza Leonardo da Vinci 32, 20133 Milano, Italy

[2] NEMAS – Center for NanoEngineered Materials and Surfaces, Politecnico di Milano, via Ponzio 34/3, 20133 Milano, Italy

[3] Department of Energy, Politecnico di Milano, via Ponzio 34/3, 20133 Milano, Italy

[4] Dipartimento di Scienze e Tecnologie Chimiche, Università di Roma Tor Vergata, via della ricerca Scientifica 1, 00133 Roma (Italy)

[5] Actinium Chemical Research srl, Via Casilina 1626A, 00133 Rome, Italy

Email: Carlo S. Casari carlo.casari@polimi.it

* Corresponding author

Abstract

Graphene, nanotubes and other carbon nanostructures have shown the potential as candidates for advanced technological applications thanks to the different coordination of carbon atoms that include the possibility of π-conjugation. In this context atomic wires constituted by sp-hybridized carbon atoms represent ideal 1-D

systems to potentially push the downscaling limit to the atomic level. In a carbon atomic wire (CAW), sp-hybridized carbon atoms can be arranged in two possible structures: a sequence of double bonds (*i.e.*, cumulenes) resulting in a 1-D metal, and an alternated sequence of single-triple bonds (*i.e.*, polyynes) expected to show semiconducting properties. In real CAWs, the electronic and optical properties can be finely tuned by controlling the wire length (*i.e.*, number of carbon atoms) and terminations (atom, molecular group or nanostructure).

Although sp-hybridized linear carbon systems are still considered elusive and unstable materials, nowadays a number of nano-systems constituted by sp-carbon wires have been produced and characterized. In this short review we present the main synthesis techniques as well as the stabilization strategies and we discuss the present status of the understanding of the structural, electronic and vibrational properties with particular attention to their close connection. We will focus on the capability of vibrational spectroscopy to provide information on the structure and electronic properties of the system (*e.g.*, determination of wire length). Moreover, by combining Raman and Surface Enhanced Raman Scattering (SERS) and with the support of first principles calculations we show that a detailed understanding of the charge transfer between CAWs and metal nanoparticles may open the possibility to tune the electronic structure from alternated to equalized bonds.

Keywords

Carbon nanostructures, Raman spectroscopy, sp-hybridized carbon systems, polyynes, cumulenes.

Introduction

In the last decades carbon nanostructures have been widely investigated for their peculiar properties and for the potential technological applications [1]. For instance, single wall carbon nanotubes represent *quasi* 1-dimensional systems whose electronic properties are strongly related to the tube structure (*i.e.*, chirality), while graphene is a 2-dimensional system with surprising electronic and optical properties [2-4]. Besides structures based on sp^2 hybridization of carbon atoms, sp-hybridized carbon atomic wires (CAWs) are intriguing systems with structure-, length- and termination-dependent properties [5]. At difference with carbon nanotubes and as a parallel with graphene, which is today considered the ultimate 2-dimensional (2-D) system (1-atom-thick), CAWs represent a true 1-D system (1-atom-large) capable to display either semiconducting or metallic properties thanks to the conjugation and electron-phonon coupling effects of their delocalized π electrons.

In addition to many examples of organic chemistry, the occurrence of sp-hybridized carbon has been observed in many carbon-based materials and structures, embedded in cold gas matrices, in free carbon clusters in the gas phase, in pure sp-sp^2 systems, in liquids, inside carbon nanotubes and connecting graphene sheets [5-13]. The research on sp carbon dates back to the last century when carbon community was looking for a new carbon allotrope based on linear carbon. The first papers claiming observations of sp-hybridized carbon as a new allotrope (named carbyne, the mineral form was called chaoite) date back to the sixties by Kudryavtsev and coworkers (published in Russian, see *e.g.*, [14]), by El Goresy and Donnay [15] and by Whittaker [16,17]. Criticisms on the interpretation of these results were raised in the eighties by Smith and Buseck and were object of debates [18,19]. In the same period the search for linear carbon in the interstellar medium for astrophysics studies

drove the discovery of fullerenes by Kroto, Smalley and Curl, as reported in the Nobel lecture by H. Kroto [20]. Even though a new allotrope based on sp carbon has still to be found, sp-hybridized carbon nanostructures (or large molecules) in the form of linear atomic wires can be now produced and investigated. A great interest has been shown in the theoretical prediction of electronic and transport properties of carbon wires connected to metal electrodes and to other carbon nanostructures such as graphene and nanotubes, while a detailed experimental work is still needed to unveil the structure and properties of these systems.

Raman spectroscopy is extremely powerful for the characterization of carbon materials and nanostructures thanks to its sensitivity to the nature of the CC bonds. For instance, electron-phonon coupling allows to measure single carbon nanostructures and together with confinement effects provide information on their structure, hybridization state, defects, presence of functionalization and/or doping, down to the determination of the nanotube chirality and the number of layers and the edge structure in graphene [21,22].

In this review we discuss how Raman spectroscopy allows to obtain a wealth of information on the structure of CAWs including length, stability behavior and electronic structure changes induced by charge transfer effects. In particular, for different CAWs, the results of a combined Raman and Surface Enhanced Raman spectroscopy investigation at different excitation wavelengths with the support of first principles calculations will be reviewed. We will start by discussing the structure of ideal and real CAWs with particular focus on π conjugation effects and the change in electronic properties as a result of the wire length and termination. Then we will review CAWs synthesis techniques and strategies to improve stability. Finally we will present Raman and SERS characterizations of selected CAW systems.

Review

Structure of carbon atomic wires

The ideal model of sp hybridized carbon wires is an infinite chain which can display two different geometric arrangements of atoms within the chain, as depicted in Figure1. One possibility is a sequence of double bonds in a completely equalized geometry (also called cumulene), the other is characterized by alternating triple and single bonds in a dimerized geometry (also called polyyne). The two configurations are physically related by stability issues since 1-D atomic equalized structures should show tendency to change into alternated ones to reach a minimum energy configuration (*i.e.*, due to the onset of a Peierls distortion). Such structural change has a direct effect on the electronic properties.

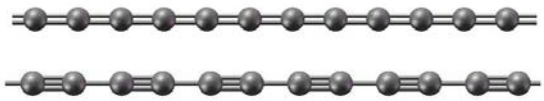

Figure 1: Schematic structures of infinite linear sp carbon wires, equalized wire with all double bonds (cumulene) and alternated single-triple bond wire (polyyne).

Infinite cumulenes have one atom per unit cell, providing 1 electron from each $2p_z$ orbital, thus forming a half-filled band of a 1-D metal. As a consequence of Peierls distortion, driven by electron-phonon coupling and dimerization of the structure, an energy gap opens and the metallic character of cumulenes changes into the semiconducting behavior of polyynes, which corresponds to a lower energy of the ideal sp-carbon chain. Along this metal-to-semiconductor transition the vibrational properties are strongly modified. One of the major effects is the appearance of one

optical phonon branch, which is otherwise absent in the equalized monoatomic infinite chain such as the ideal cumulene.

Moving from ideal to real structures, finite length effects and terminations play a fundamental role. The end groups can affect the overall configuration and their effect is increasingly larger with decreasing the wire length. The control of the electronic properties such as the gap and the conducting character by tuning of the wire structure may thus open new perspectives for the realization of nanoscale cables and devices, as shown by theoretical predictions (see *e.g.*, [23,24]) but still not experimentally demonstrated. Indeed, this possibility exploits the connection existing between the molecular structure, the electronic properties and also vibrational properties which is well documented for all π-conjugated carbon systems [25-28]. The infinite wire model affords a reliable interpretation of the experimental data, capturing the main trends observed in both electronic and vibrational features and offering a unified framework for the analysis of the different linear carbon chains synthetized till now. Indeed, many works [28-34] have offered a detailed theoretical interpretation of the links existing among chain structure, band gap and Raman activity of the infinite chain, thus fostering the interpretation of the behavior of the existing finite length carbon chains. However, this approach may also show some limitations due to non-negligible end-effects which may require the relaxation of the assumption of an infinite atomic chain for the detailed discussion, in real finite-length systems, of Peierls distortion effect, stability of cumulenic *vs*. polyynic chains and vibrational structure (*i.e.*, IR and Raman signals). Starting from the structural properties, the most significant parameter in this context is the Bond Length Alternation (BLA) *i.e.*, the difference between the average length of “quasi”-single and “quasi”-triple bonds in the chain: it is well-known that the increase of the length of the sp (or sp^2) carbon chain induces an increase in π-electron conjugation,

corresponding to a BLA decrease [25, 27, 35-38], as easily rationalized by straightforward application of Hückel theory. Therefore, longer chains will show a "more" equalized structure with a smaller BLA [26,29, 30, 38-41], even if the occurrence of Peierls distortion would make unstable the perfectly equalized chain. On this basis, the markedly polyynic structure found in most of the synthetized sp-carbon chains has been usually related to the influence of Peierls distortion. Indeed, BLA decreases with increasing chain length (π-conjugation) for both polyynes and cumulenes (see Figure2), similarly to many other polyconjugated materials. However, a detailed computational analysis on long sp-carbon chains [41] clearly demonstrated that Peierls distortion contrasts the decrease of BLA caused by the increasing degree of π-electron delocalization only in long enough chains: it has been verified that C_n chains possess a cumulenic structure determined by end-effects for $n < 52$, while in longer sp-chains the onset of Peierls distortion imposes an alternated structure. This is consistent with the fact that Peierls distortion may be rigorously defined just for an infinite chain. Hence in shorter sp-chains the presence of end-effects cannot be overlooked [40, 41] and the structure (BLA) of finite sp-chains is determined mainly by the chemical nature of the end-capping groups. In Figure2 BLA and CC bond lengths (computed with DFT) are reported for a selection of differently capped sp-chains [39]. In hydrogen-capped chains, the H- terminal forces the formation of a triple bond on the adjacent CC bond, so that a single bond is formed on the next CC bond, thus inducing a polyynic structure. On the other side, a vinylidene cap (*i.e.*, $=CH_2$) induces a double CC bond on the sp-chain end, thus promoting a much more equalized, cumulene-like, structure. For the same number of C atoms in the sp-chain, vinylidene-capped chains exhibit a much more equalized structure with respect to hydrogen-capped chains, highlighting that the geometry of finite sp carbon chains is not dictated by Peierls distortion but it is completely due to end-effects. This property

paves the way to the design of new sp-carbon compounds where, by a proper choice of the end groups, it is possible to modulate the chain structure, possibly down to very low BLA, thus forming structures that can be practically considered cumulenic. By consequence the electronic properties of the conjugated system can be modulated from a semiconductive to a metallic behaviour. On these grounds, the recent works by Tykwinski *et al*. [42, 43] are particularly meaningful. Long sp-carbon chains, containing up to 9 cumulated C=C bonds have been synthesized by a proper choice of the end-capping groups. They represent, to the best of the authors knowledge, the first long cumulenes obtained by rational chemical synthesis.

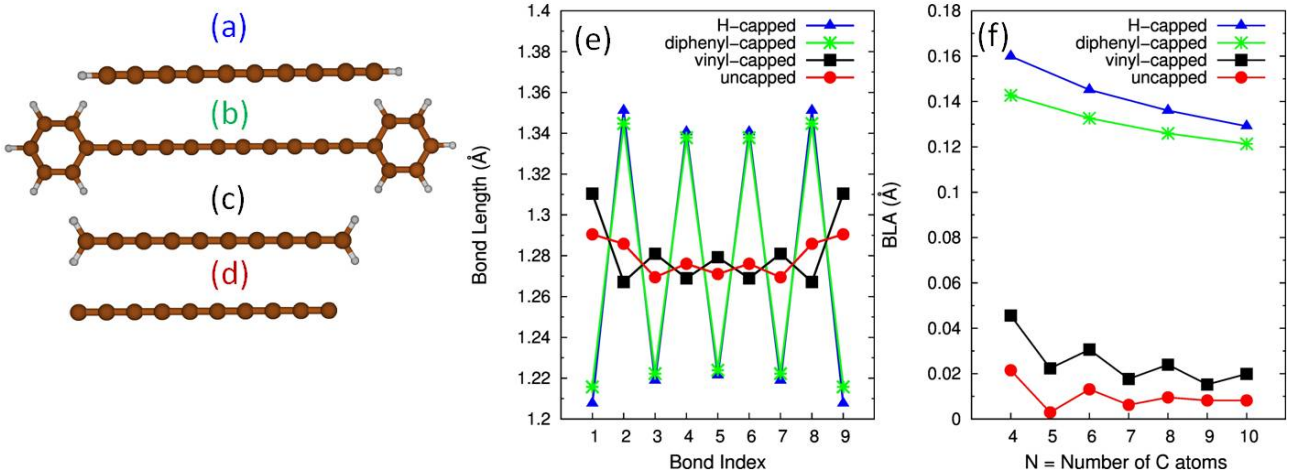

Figure 2: (a-d): carbon atomic wires with different terminations: Hydrogen-capped (a), phenyl-capped (b), vinyl-capped (c) and uncapped (d). The bond length and the bond length alternation (BLA) as a function of the number of carbon atoms composing the wire are reported in panels (e-f). Data are from DFT calculations.

Synthesis techniques and stability strategies

Different techniques, both physical and chemical, can be used to produce sp carbon wires in several forms, mainly in a bottom-up approach [5]. Physical techniques are mainly based on the rapid quenching of a carbon vapor in different environments.

Supersonic carbon cluster sources based on the arc discharge between graphite electrodes (*i.e.*, pulsed microplasma cluster source – PMCS developed by P. Milani and co-workers) demonstrated the capability to produce sp-sp^2 hybrid amorphous carbon films with estimated sp content up to 40% [44, 45]. Unfortunately the sp phase easily undergoes rearrangement to the sp^2 phase when the sample is exposed to air due to oxidative and cross linking effects and thus requires *in situ* characterization techniques, as reported in many papers *e.g.*, [7, 46]. A similar approach was exploited using thermal or laser vaporization cluster sources [6, 47]. Sp carbon has been also produced by ion irradiation of amorphous carbon [48] and by femtosecond (fs) laser irradiation of a graphite target [49]. fs laser pulses have been used to produce amorphous carbon films containing sp, sp^2 and sp^3 fractions, while no control over their relative amounts has been shown [50]. Isolated wires can be produced by laser ablation (with both fs and ns pulses) of carbon solid targets or suspensions in liquids and particularly in the polyyne-like form with an even number of carbon atoms [7,45]. With reference to polyynes in solution an easy-to-use and cost-effective technique is the arc discharge in liquids developed by F. Cataldo [51]. This technique also allows controlling the chain termination by selecting suitable solvents [52].

Different chemical techniques have been used to synthesize a large number of sp carbon chains terminated with different molecular groups as reported in the review by Szafert and Gladysz [53]. Among the most employed chemical routes we cite: dehydropolycondensation of acetylene, the Glaser reaction based on the oxidative coupling reaction of ethynyl groups by copper salts; polycondensation reactions of halides; dehydrohalogenation of polymers such as the chemical carbonization of poly(vinylidene halides) (PVDH). Wire formation via self assembling of carbon atoms

in the presence of Pt atoms on graphene has been recently reported by Kano et al. [54]

With reference to top-down methods the only technique proposed so far is represented by electron bombardment sometimes even combined to axial strain of a carbon nanotube [55] or of a single graphene flake in a TEM thus allowing to selectively remove carbon atoms until a single atomic chain is formed as a junction between nanotubes or connecting two separate graphene edges [13]. Other systems of carbon wires connected to graphene edges have reported by some authors (see e.g. [56-58])

One of the major problems arising when synthesizing sp carbon wires is the stability of the structures. A viable route to the synthesis of stable structures is the stabilization of already formed wires and a few attempts have been made in this direction so far. We demonstrated that H-terminated polyynes could be embedded in a solid assembly of Ag nanoparticles resulting in a sample stable for several weeks at room temperature and in air conditions [59]. Hayashi and co-workers showed that it is possible to produce a polymeric composite (*i.e.*, poly(vinyl alcohol)) containing polyynes stabilized by Ag nanoparticles [60].

Thanks to their higher stability, polyynes in liquids (up to 14-16 carbon atoms) are nowadays synthesized even in the form of size-selected samples [5, 61, 62] and with well-defined end groups [53]. Solid-state samples have been also produced in powder form [63] and recently Chalifoux and Tykwinski reported the synthesis of chains up to 44 carbon atoms terminated by bulky groups [64]. The latter system is stable in air and at room temperature in the form of a solid sample. On the contrary cumulenes seem more difficult to produce and fewer works are present reporting their observation. For instance both cumulenes and polyynes have been detected in a pure sp-sp^2 cluster-assembled system [9,65] and the higher tendency of cumulenes

to undergo sp^2 transformation has been outlined [44, 66, 67]. By playing with termination-induced electronic arrangement, short cumulenic structures can be produced, as reported by Cataldo [68] and extensively discussed in the review by Cadierno et al. [69]. A significant step in the preparation of long cumulenic chains has been very recently presented by the group of Tykwinski [42,43]: by adopting different synthesis procedures, long cumulenes chains (up to 8 sp carbon atoms) have been selectively obtained. Again, the end caps play a fundamental role for two reasons. On one hand, due to their chemical nature, they promote the formation of a double bond on the first bond of the sp chain, as required to induce a cumulenic structure. On the other hand, they are chosen bulky enough to prevent interactions among sp chains thus avoiding cross-linking and degradation.

Raman spectroscopy of carbon atomic wires

As pointed out when discussing structural and electronic properties, also for the vibrational properties (notably Raman activity [70, 71]), CAWs share the same characteristics of other one-dimensional polyconjugated carbon systems, such as polyacetylene and polyenes. The Raman spectra of these π-electron systems have been extensively investigated (see for instance [25, 27, 35-37] and references therein) and show a peculiar behaviour. In particular the dominant feature is originated by oscillation of the BLA that is an out-of-phase CC stretching and is named "*R* mode" or "ECC mode" according to the Effective Conjugation Coordinate (ECC) model [25, 27, 35, 36].Such spectral line is characterized by decrease of wavenumbers and increase of intensity with increasing the wire length (i.e. number of carbon atoms). In addition, recent theoretical analysis carried out with DFT methods suggests that, for long wires and under axial strain along the sp-chain, anharmonicity

may also drastically affect the Raman spectra, with an interesting interplay with Peierls distorsion effects [72].

Examples of the extreme sensitivity of Raman spectroscopy to the carbon hybridization state, electronic structure and local order, are shown in Figure 3 where different carbon systems are characterized by well-defined Raman features. At difference with respect to the case of other allotropic forms of carbon (*e.g.*, fullerenes, nanotubes, graphene), the Raman spectroscopy of sp carbon chains has been investigated in detail only recently and a consistent description just begins to emerge. The Raman spectrum of polyynes shows a similar behaviour to polyenes with a very intense line that has been called “α line” by some authors [61] and corresponds to the *ECC* mode. In addition a second, minor band (β line) is often observed. All these fingerprints fall in the 1800-2300 cm^{-1} region and they are related to different collective stretching vibrations of sp hybridized CC bonds (*i.e.*, BLA oscillation modes), which have been discussed in detail in [31] through theoretical analysis and first-principles calculations. This spectral region turns out to be specific for sp carbon since none of all the other carbon nanostructures have peaks in this region (see Figure 3). Within this spectral region cumulenes exhibit an overall lower frequency Raman signals than polyynes.

DFT calculations have quantitatively shown that for realistic systems with finite length the strong electron-phonon coupling is responsible for the red-shift of the Raman mode when increasing the length. [30, 32, 34,40].

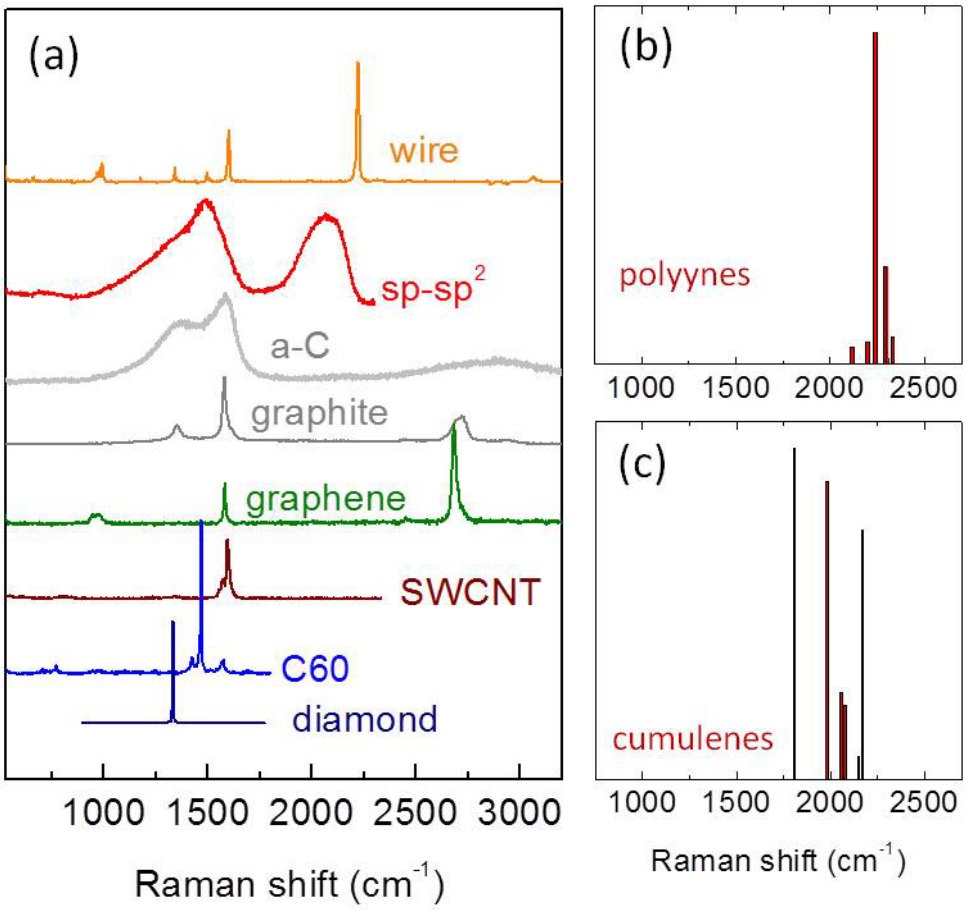

Figure3: (a) Experimental Raman spectra of carbon solids and nanostructures. (b-c) DFT computed Raman peaks for finite polyynes and cumulenes of different lengths (PBE0/cc-pVTZ, from [39]).

Furthermore, a first interpretation has been carried out by taking into account the infinite chain model which allow to interpret the α and β lines on the basis of the Longitudinal Optical (LO) phonon dispersion branches of an infinite, Peierls distorted, carbon chain (*i.e.*, with two atoms in the unit cell). Similarly to the case of the electronic structure, where the band gap is modulated by BLA, showing a transition from semiconductive states (BLA ≠ 0) to the metallic state (BLA = 0), also the LO phonon branch is strongly modulated by BLA and it shows a Kohn anomaly at Γ in the case of a cumulenic chain [29, 30-32,34]. This behaviour can be interpreted on

the basis of the modulation of the *ECC* mode force constant driven by the occurrence of increasingly more extended π-electron delocalization for decreasing BLA. This point has been theoretically demonstrated by means of Hückel theory [28, 31, 32], which allows highlighting the important role of long-range vibrational interactions among CC stretching coordinates in the sp-carbon chain. As in the case of standard polymer systems, the wavenumbers associated to LO vibrations in finite length chains may be placed on the LO branch of the respective infinite model at different points of the first Brillouin zone. This procedure, reported in details in refs [32, 71], consists in analyzing the displacement vectors associated to CC stretching normal modes, finding the nodal pattern and associating the corresponding phonon wavevector. For polyynes the ECC modes of a finite chain characterized by a given BLA can be put in correspondence with the LO dispersion branch obtained for the same BLA value. This ideal model can be successfully adopted to give an interpretation of the Raman spectra of hydrogen-capped chains of increasing lengths [29, 30] and long polyynes (containing up to 20 conjugated triple bonds) capped with bulky groups [71]. The same approach also allows describing the Raman spectra of cumulenic species [39]. The latter case is particularly interesting since it highlights the inherent weakness of the infinite chain model. The possibility of detecting cumulenic chains by Raman spectroscopy has been often contrasted by some author based on the fact that an infinite chain with equivalent double bonds would be a monoatomic chain with no optical phonon branch. However, the existence of cumulenic molecular systems has been suggested by Raman spectroscopy for mixed sp/sp^2 carbon nanostructures [9,46,65]. This apparent contradiction can be solved by relaxing the infinite chain model. While only phonons at Γ have a non negligible Raman activity for an infinite polymer, for finite chains also vibrations located on the LO branch at different points of the 1^{st} Brillouin zone can be Raman active, thanks to

end effects (which obviously lack when periodic boundary conditions are assumed). For instance, the Raman spectra of several cumulenic (C_n) chains, computed by DFT are reported in [39]. Many vibrational transitions show non negligible Raman intensity, thus demonstrating the possibility of detecting cumulenic chains by means of Raman spectroscopy. Interestingly, the interplay between the activation of out-of-Γ normal modes and the molecular parameters governing Raman activity [28, 73] generates in cumulenes a detectable Raman signal also for LO modes other than ECC, as shown in Panels (b) and (c) of Figure 3. Still with reference to cumulenes, it has to be noticed that Liu et al. reported that finite cumulenes have a well-defined torsional stiffness, which brings about the possibility to consider relative twisting vibrations of the CH2 endgroups as potential Raman signals useful for the characterization of these systems, since their respective force constant decreases as 1/length [74]. To this respect , however, calculations of the Raman response of these modes [39] have revealed that such modes are expected to be very weak (or inactive) compared to bending modes which occur in a close wavenumber range and have been observed in [66], thus hindering the possibility to detect these CH2 twisting modes by Raman spectroscopy.

Based on the above discussion, it should be clear how end-effects might affect the overall properties of sp-carbon chains, not only by modifying the molecular structure (*i.e.*, BLA) but also influencing the electronic and vibrational properties. By properly choosing the end-groups one can modulate the structure of the chain with the aim of modulating the band gap of the system; this effect can be spectroscopically probed thanks to the evolution of the distinct marker bands observed in the Raman spectra. Hence Raman spectroscopy, enhanced by the strong predictive power of first-principles simulations, constitutes a powerful non-invasive characterization technique, which can provide valuable information on the molecular properties of sp-

carbon systems. This may prove to be useful in nanotechnology application scenarios.

We would like now to introduce a few case studies where Raman spectroscopy proved to be particularly insightful to characterize sp-carbon systems. For two cases (hydrogen- and phenyl-terminated polyynes) we will show that Raman spectroscopy allows identifying CAWs of different lengths. Furthermore, by comparing Raman and SERS we will discuss the occurrence of charge transfer between CAWs and metal nanoparticles used as the SERS active substrate. Such charge transfer results in a change of the electronic configuration of the wire that evolves towards a more equalized structure (*i.e.*, cumulenic).

H-terminated polyynes were produced by the submerged arc discharge technique, as described in detail in [64]. When the discharge is operated in methanol it is possible to obtain polyynes with an even number of carbon atoms ($6 \leq C \leq 16$) terminated by one hydrogen atom on each side. The size distribution obtained from HPLC complemented with UV-Vis spectroscopy is reported in Figure 4. Even at low concentration it is possible to obtain a Raman spectrum from the liquid sample as shown in Figure 4(a) where the low intensity of the sp signal is clear when compared to the signal of the solvent (methanol). The sp signal forms an asymmetrical band extending from 2000 cm^{-1} to 2250 cm^{-1} as a result of the contribution of wires of different lengths.

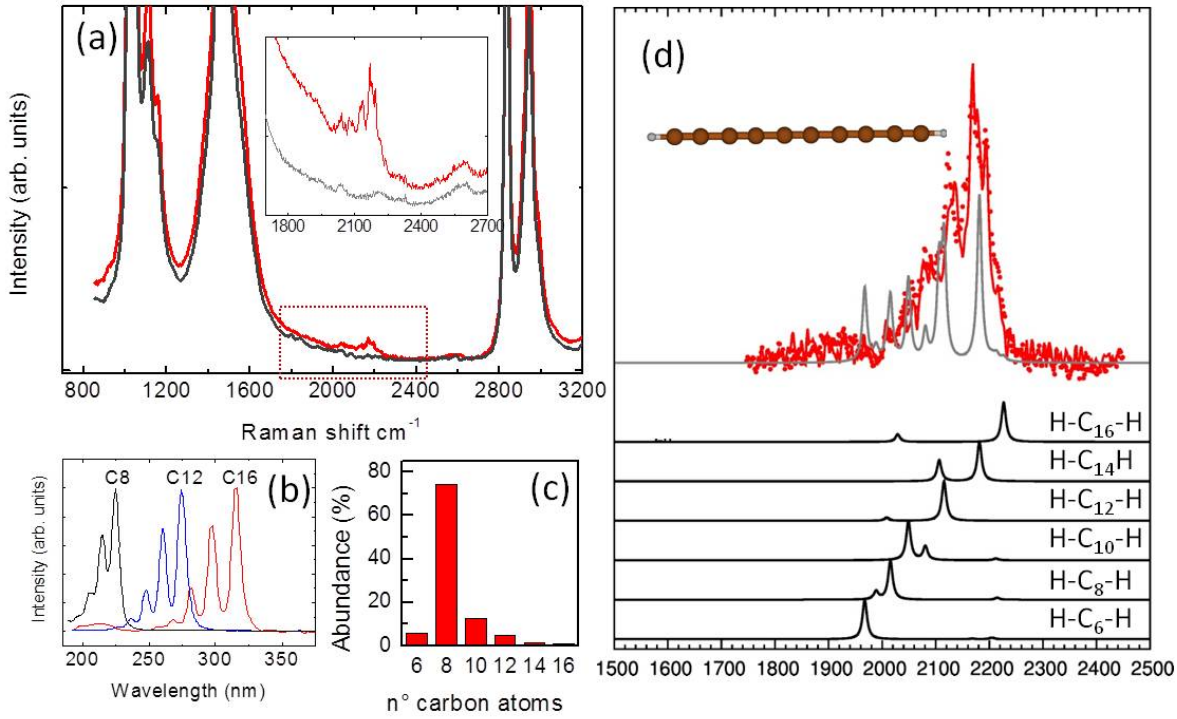

Figure4: (a) Experimental Raman spectrum (1064 nm) of H-capped polyynes in methanol solution ($5x10^{-3}$ M), the solvent alone is shown for comparison. (b-c) UV-vis spectra for polyynes of different lengths and size distribution in the sample solution. (d) DFT computed Raman peaks for polyynes present in the sample weighted by their correspondent abundance and comparison with the experimental spectrum. Adapted with permission from [75].

As already mentioned the vibrational features are strongly dependent on the wire length and this is clearly shown in the theoretical spectrum obtained by computing the active Raman modes with their intensity for single wires with a number of carbon atoms the range 6-18. The frequency of the Raman modes is decreasing for longer wires while the Raman intensity increases. Although the correct Raman intensity behaviour as a function of chain length is not very accurately captured by DFT methods, by summing up the different contributions, weighted by their abundance in

the sample, we can obtain a fair representation of the experimental spectrum. Hydrogen terminated polyynes show a limited stability in time since they easily undergo a transition towards sp^2 as a consequence of cross-linking reactions [76]. It is known that bulkier end groups than hydrogen, such as phenyls or even bigger caps [64], impart stability to CAWs. Phenyl terminated polyynes were produced by chemical synthesis; details are given in [77]. Thanks to the termination these systems are stable at ambient conditions even when the solvent is completely removed and the sample is in the solid state, as shown in Figure 5. The Raman spectrum of diphenyl-polyynes is characterized by well-resolved peaks in the 2050-2250 cm^{-1} region. Also in this case, this is due to a size distribution of polyynes in the sample. This is confirmed by the spectrum of the size-selected sample with 4 carbon atom wires. The additional peak at 1600 cm^{-1} is related to the stretching of the phenyl ring, hence it is a marker of the termination with sp^2 character.

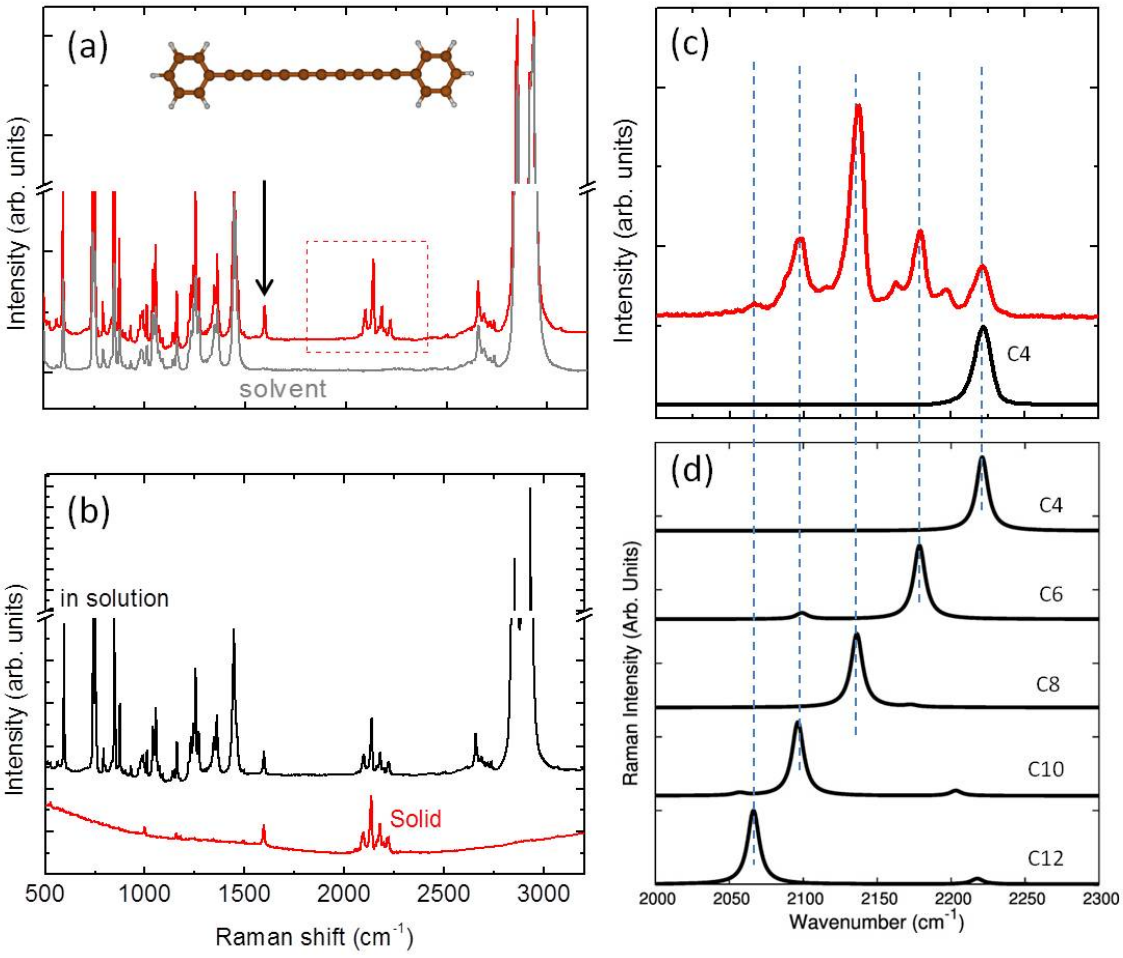

Figure5: (a) Experimental Raman spectrum (1064 nm) of phenyl-capped polyynes in decalin solution (10^{-2} M), the solvent alone is shown for comparison. The peak from the phenyl termination is marked with an arrow. (b) Raman spectrum of phenyl-capped polyynes after solvent removal to show stability of the sample. (c) Detail of the experimental Raman spectrum of panel (a). The spectrum of size-selected phenyl –capped polyyne with 4 carbon atoms is also reported. (d) Peaks of different wire lengths according to DFT calculation of the Raman modes (PBE0/cc-pVTZ, from [38]). Adapted with permission from [38]. Copyright 2011 American Chemical Society.

DFT calculations of the Raman spectra of several phenyl-capped polyynes of selected length allow assigning each observed peak to a given size of the sp-chain. In this case also we observe a significant red shift of the ECC mode for increasing chain lengths, which is consistent with the increase of π conjugation. The Raman intensities of the computed spectra reported in panel (d) of figure 5 are normalized to allow a better comparison with the experimental spectra.

A peculiar effect is observed when polyynes (both H- and phenyl-terminated wires) interact with metal nanoparticles (*i.e.*, silver and gold), such as those employed in Surface Enhanced Raman Scattering (SERS) to increase the sensitivity of the Raman technique. Interaction with metal nanoparticles has been investigated both in solution and on a surface. SERS in solution has been carried out by adding silver and gold colloids to the sample solution while for Surface SERS (S-SERS) silver and gold nanoislands supported on silicon and glass substrates have been used [38]. We observe that the SERS spectrum is radically different from the Raman spectrum. A shift of the main Raman feature is accompanied by the appearance of new spectral features at lower wavenumbers (*i.e.*, below 2000 cm^{-1}), as shown in Figure 6 for the case of silver nanoparticles. This happens also in the case of gold nanoparticles for different excitation wavelengths ranging from NIR to blue wavelength (1064 nm to 458 nm), showing that it is not a resonance-activated effect [38].

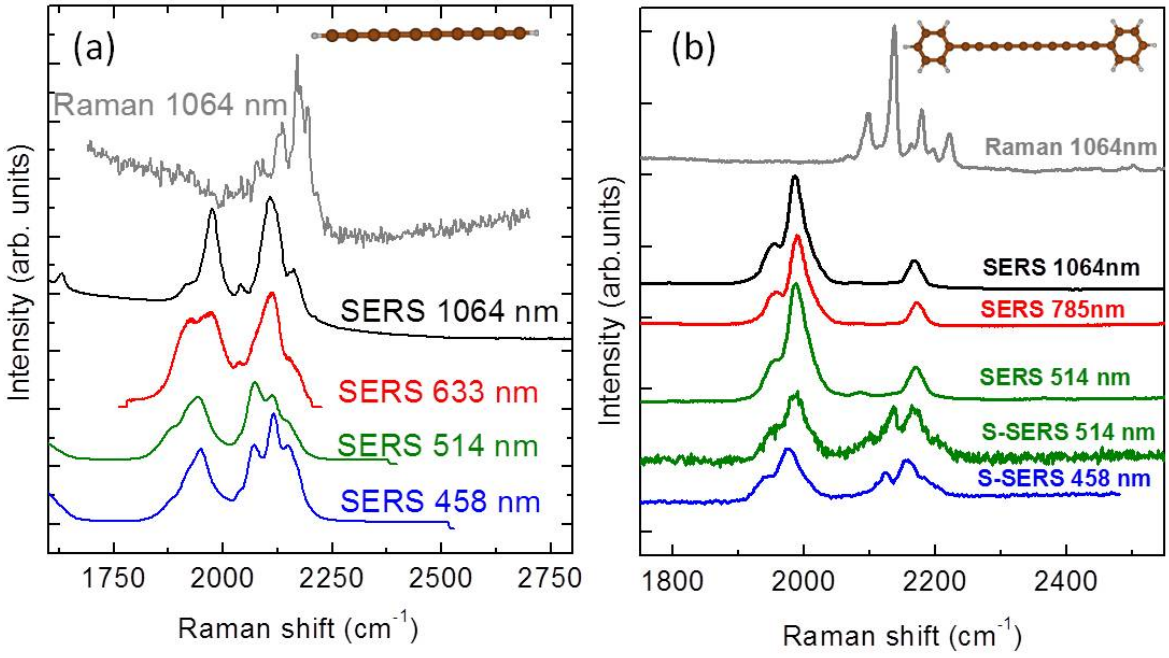

Figure6: (a-b) SERS spectra of H-capped and phenyl-capped polyynes in solution at different excitation wavelengths. SERS on solid surfaces (S-SERS) of phenyl-capped polyynes are also reported. The Raman spectra (1064 nm) of both systems are shown for direct comparison. Adapted with permission from [38]. Copyright 2011 American Chemical Society.

When interacting with metal nanoparticles in solution, H-terminated polyynes promote colloid aggregation, which causes the plasmon resonance to shift from the visible and broaden, thus extending to the NIR. This effectively allows performing SERS with different excitation wavelengths. This behavior of H-terminated polyynes can be rationalized by assuming a strong chemical interaction with metal particles and even substitution of the hydrogen with silver. This effect can also justify the increased stability that we have observed after the mixing with silver nanoparticles [59]. Phenyl-capped polyynes show a similar aggregation when mixed with metal nanoparticles.

The modifications occurring in the vibrational properties of wires upon interaction with metal nanoparticles (*i.e.*, observed comparing Raman with SERS) suggest a chemical SERS effect with total enhancement factors up to 10^6 as observed in the case of H-capped polyynes [75]. In order to explain this observation, the possibility of a charge transfer between the metal and the carbon wire has been proposed [38]. Computing the Raman frequency of CAWs of different lengths and comparing neutral CAWs with charged ones it is straightforward to observe a relevant softening of the ECC Raman modes and an increase of their Raman activity which is promoted for larger conjugation, as reported in Figure 7.

For instance, for a wire of given size a decrease of about 100 cm^{-1} is predicted when the wire is charged, both by adding or removing one electron. The trend in both frequency and Raman intensity is similar even though the shifting effect is slightly different upon oxidation/reduction in long/short chains. By consequence, either in the case of positively or negatively charged diphenyl-capped polyynes, new bands would appear in the spectra at lower wavenumbers and with a larger Raman activity, which can explain the recorded experimental SERS spectra.

To understand the direction of the charge transfer an energy balance is required.

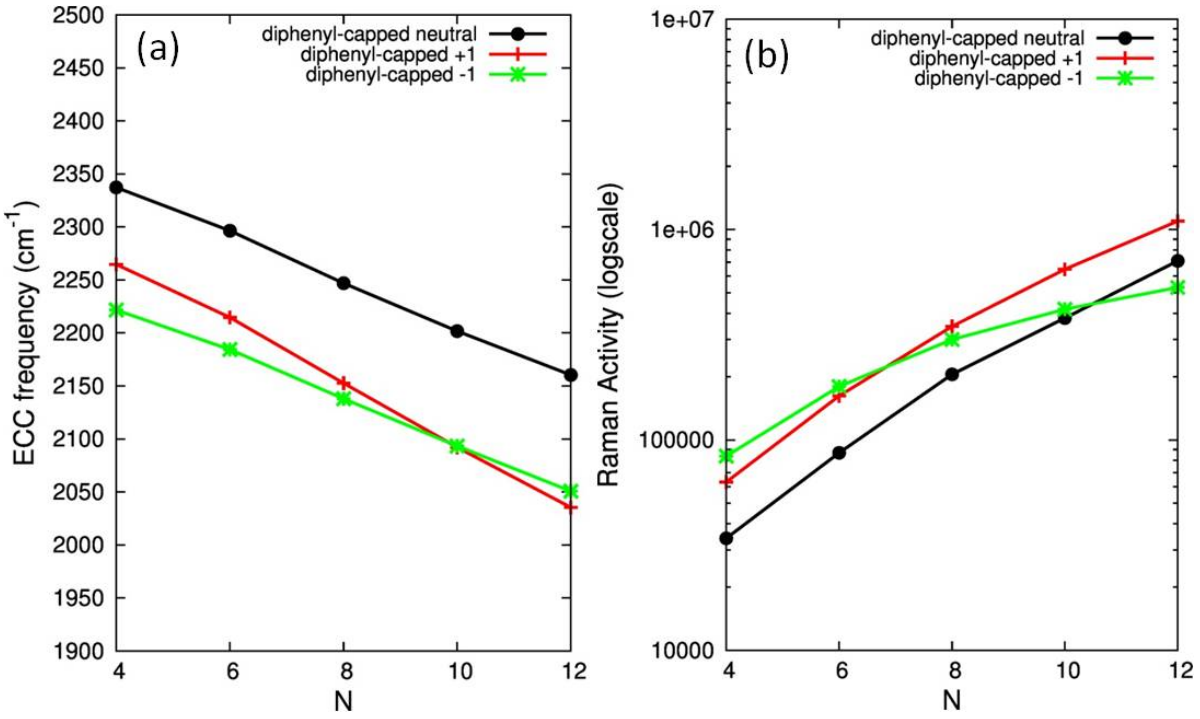

Figure 7: (a-b) Modulation of the DFT computed (PBE0/cc-pVTZ, from [38]) vibrational frequency and Raman activity of the ECC band for phenyl-capped polyynes of different lengths (N) and charge states (0, +1, -1). Adapted with permission from [38]. Copyright 2011 American Chemical Society.

Figure 8(a) reports for each wire length the energy E^{ion} required for the formation of the two possible charged configurations, namely Ag^{+} $[Ph\text{-}C_n\text{-}Ph]^{-}$ and Ag^{-} $[Ph\text{-}C_n\text{-}Ph]^{+}$. Given a pair of ionic species A+..B-, E^{ion} is defined as E^{ion} = IP(A) - |EA(B)|, where IP(A) is the ionization potential of A and EA(B) is the electron affinity of B. By evaluating this term for the two charged configurations indicated above we can determine the direction of the charge transfer since the complex possessing the lower value of E^{ion} would be preferentially formed.

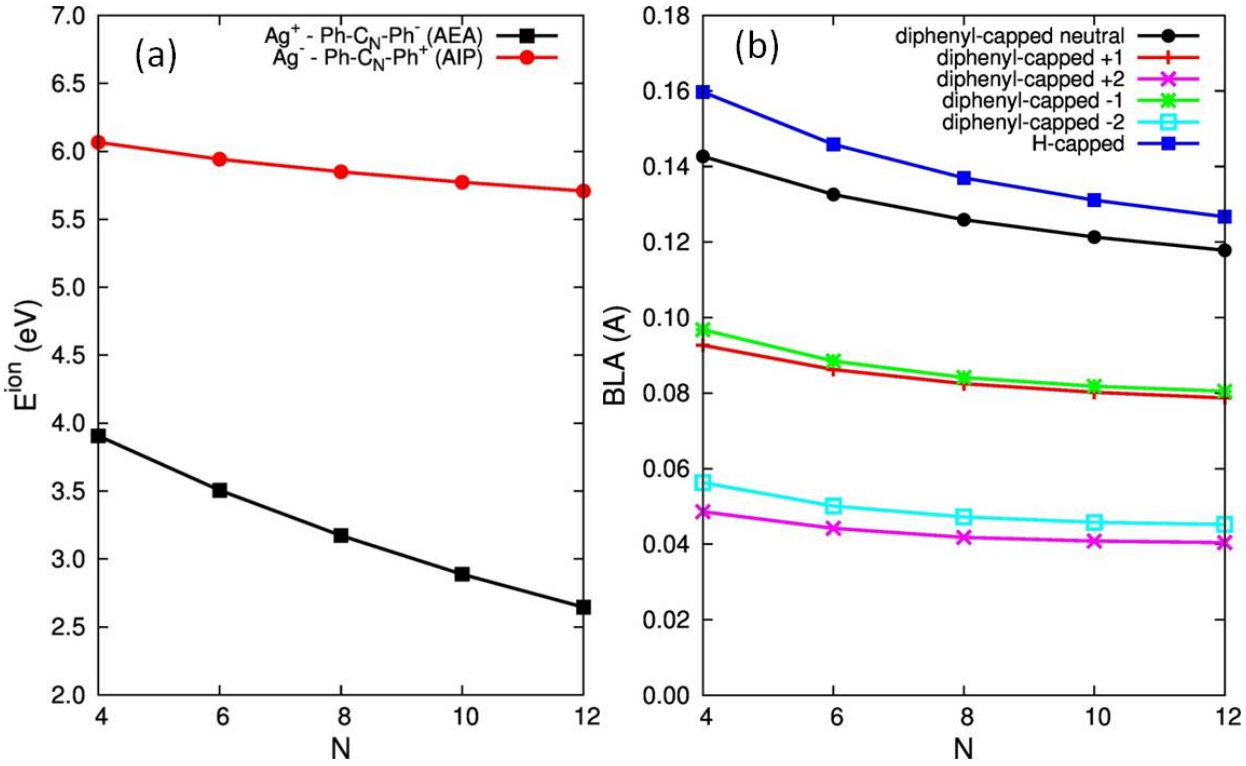

Figure8: (a) Plot of the DFT computed work (PBE0/cc-pVTZ, from [38]) required for the formation of the charged species (E^{ion} = IP(A) - | EA(B) | where IP is the ionization potential of A and EA is the electron affinity of B) for the two possible cases Ag+ • [Ph-CN-Ph]- and Ag- • [Ph-CN-Ph]+ of phenyl-capped polyynes of different chain lengths (N). Experimental values of work function and EA has been used in the case of Ag: IP=4.6 eV and EA =-1.30 eV for EA [34] (b) Modulation of the DFT computed (PBE0/cc-pVTZ, from [38]) BLA for phenyl-capped polyynes of different lengths (N) and charge states (0, +1, -1). Adapted with permission from [38]. Copyright 2011 American Chemical Society.

IP and EA have been calculated for neutral and charged diphenyl-capped polyynes: in particular "adiabatic" IP (AIP) and EA (AEA) are reported by considering the total energy of the charged species in their minima, thus including geometry relaxation

effects upon charge transfer. For Ag we have considered the experimental values of IP and EA [38].

Based on this calculation and panel (a) of Figure 8 it is clear that the configuration with a positively charged metal and negatively charged wire is favored. Furthermore, also in this case the trends of E^{ion} are modulated by π conjugation. For increasing chain lengths (*i.e.*, larger conjugation) the energy required for the formation of charged species decreases, thus favoring the charge transfer process.

In addition, since charge transfer obviously alters the electronic structure of the wire, we can expect some effect also on the molecular structure. This is due to the characteristic and strong electron-phonon coupling existing in π-conjugated systems which connects the electronic effects with the structure of the sp-chain. This indeed happens, as demonstrated by the BLA values computed for the neutral and charged species and shown in Figure 8(b). Charge transfer induces a BLA decrease in the polyyne structure, which evolves towards a more equalized structure. In other words, upon charge transfer the wire moves from alternated (polyyne) to equalized (cumulene) wire configuration. The reduction amounts to more than 30% for a singly charged wire and more than 60% for a doubly charged wire, reaching a lower value of 0.04 Å for 12 carbon atoms. It is important to notice that for finite-length wires the ideal cumulene structure with BLA = 0 Å is not realistic due to the influence of the terminations. The end effects are stronger in shorter wires, as in Figure 2-f where the BLA of finite cumulenes is reported. Vinylidene-capped systems have a BLA which ranges from about 0.05 Å to 0.02 Å moving from 4 to 10 carbon atoms. Uncapped C_n cumulenes show a BLA below 0.02 Å even though they represent a model system that is experimentally unfeasible, except in extreme conditions. As a reference, this result agrees with theoretical calculations by Weimer et al. [78] reporting an increase

in the BLA in cumulene wires from 0.006 to 0.048 when the chain length is decreased from 40 to 4 atoms.

This approach gives a qualitative evaluation of the charge transfer since it is not including in the calculation the effect of wire-to-metal interaction. The proposed effect is reasonable even though a more complete model should consider the whole wire and metal system and their interaction. This is indeed extremely complex and time consuming from the calculation point of view due to the large numbers of atoms and the need of considering electronic and vibrational properties.

Conclusions

Sp carbon atomic wires show appealing properties for fundamental studies and applied research. They represent an additional player in the family of carbon nanostructures and can be potentially integrated with graphene and nanotubes to take advantage of the large tunability of electronic and optical properties. We have here reviewed the present understanding of structure-property relationship and the use of Raman and SERS for a detailed investigation of wire structure and electronic properties. Stable polyynes can be today synthesized while for technological applications additional work is needed to reveal the properties of wires assembled in thin films. Cumulenes are particularly appealing as a 1-dimensional metal even though the synthesis is still challenging. Another strategy in this direction is represented by modifying the structure of polyynes through the control of charge transfer effects.

Sp carbon has also attracted interest as a molecular junction, as shown in a number of theoretical investigations and a few experimental works about wires connected to graphene and nanotubes, showing interesting electronic and transport properties [79-

83]. While experimental works are still focused on the synthesis and structural investigation of different CAWs, mixed sp-sp^2 systems are attracting the carbon community as hypothetical novel hybrid carbon allotropes [84]. Among possible sp-sp^2 hybrids theoretically predicted we mention graphyne systems, as outlined by A. Hircsh [1]. Such structures are 2-dimensional carbon layers where sp^2 rings form a network through sp linear connections. For some of these systems peculiar properties are expected such as the existence of Dirac's cones in the electronic band structure and extremely high electron mobility (see e.g. [85]).

References

[1]. Hirsch A. Nature Mat. **2010**, 9, 868.

[2]. Avouris Ph. Physics Today January **2009** 34.

[3]. Novoselov K.S., Falko V.I., Colombo L., Gellert P.R., Schwab M.G., Kim K. Nature **2012**, 490, 192.

[4]. Ahn J-H. and Hong B.H. Nature Nanotechnology **2014**, 9, 737.

[5]. *Polyynes Synthesis, properties and Applications,* Cataldo F. Ed. Taylor and Francis **2006**.

[6]. Wakabayashi T., Ong A-L, Strelnikov D., Kraetschmer W., J. Phys. Chem. B **2004,** *108*, 3686-3690.

[7]. Ravagnan L., Mazza T., Bongiorno G., Devetta M., Amati M., Milani P., Piseri P., Coreno M., Lenardi C., Evangelista F.,Rudolf P. Chemical Communications **2011,** *47*, 2952-4.

[8]. Zaidi A.A., Hu A., Wesolowski M.J., Fu X., Sanderson J.H. , Zhou Y., Duley W.W., Carbon **2010**, *48*, 2517-2520.

[9]. Ravagnan L., Siviero F., Lenardi C. P. Piseri, Barborini E., Milani P., Casari C.S., Li Bassi A., Bottani C.E., Physical Review Letters, **2002**, *89*, 285506.

[10]. Tabata H., Fujii M. and Hayashi S., Carbon **2006**, *44*, 522-529.

[11]. Tabata H., Fujii M. and Hayashi S., Chem. Phys. Lett. **2006**, *420*, 166.

[12]. Zhao X., Ando Y., Liu Y. Jinno M, Suzuki T. Physical Review Letters **2003**, *90*, 187401.

[13]. Jin C., Lan H., Peng L., Suenaga K., Iijima S. Physical Review Letters **2009**, *102*, 205501.

[14]. *Carbyne and Carbynoid structures*, Heimann R.B., Evsyukov S.E., Kavan L. Eds, Kluwer **1999**

[15]. El Goresy A. and Donnay G. Science **1968**, *161*, 363.

[16]. Whittaker A.G., Kintner P.L. Science **1969**, *165*, 589.

[17]. Whitteker A.G. Science **1978**, *200*, 763.

[18]. Smith P.P.K., Buseck P.R. Science **1982**, *216*, 984

[19]. Whittaker A.G. Science **1985**, *229*, 485 and Smith P.P.K., Buseck P.R. Science **1985**, *229*, 486.

[20]. Kroto H. Rev. Mod. Phys., **1997**, *69*, 703.

[21]. Malard L.M., Pimenta M.A., Dresselhaus G. , Dresselhaus M.S. Physics Reports **2009**, *473*, 5187.

[22]. Ferrari A.C., Solid State Communications **2007**, *143*, 47–57.

[23]. Lang N.D. and Avouris Ph., Physical Review Letters **2000**, *84*, 358.

[24]. Tongay S., Senger R., Dag S., and Ciraci S., Physical Review Letters **2004**, *93*, 136404.

[25]. Zerbi G., in “Vibrational Spectroscopy of Polymers: Principles and Practice”, Eds: Everall N.J., Chalmers J.M., Griffiths P.R., Wiley, Chichester, 2007 p. 487-537 and references therein.

[26]. Kertesz, M.; Choi, C.H.; Yang, S.J. Chemical Reviews, **2005**, *105(10)*, 3448 – 3481.

[27]. Del Zoppo M., Castiglioni C., Zuliani P., Zerbi G., in “Handbook of Conductive Polymers 2nd Ed.”, (Eds: Skotheim T., Elsembaumer R.L., Reynoilds J.), Dekker, New York, **1998**, 765.

[28]. Milani, A.; Tommasini, M.; Zerbi, G. J. Raman Spectrosc. **2009**, *40*, 1931.

[29]. Milani A., Tommasini M., Del Zoppo M., Castiglioni C., Zerbi G., Phys. Rev.B **2006**, *74*, 153418.

[30]. Tommasini M., Fazzi D., Milani A., Del Zoppo M., Castiglioni C., Zerbi G., J. Phys. Chem. A **2007**, *111*, 11645.

[31]. Tommasini M., Milani A., Fazzi D., Del Zoppo M., Castiglioni C., Zerbi, G. Physica E, **2008**, *40*, 2570.

[32]. Milani A., Tommasini M., Zerbi G., J. Chem. Phys. **2008**, *128*, 064501.

[33]. Tommasini M., Fazzi D., Milani A., Del Zoppo M., Castiglioni C., Zerbi G. Chem. Phys. Lett. **2007**, *450*, 86.

[34]. Milani A., Tommasini M., Fazzi D., Castiglioni C., Del Zoppo M., Zerbi G., J. Raman Spectrosc. **2008**, *39*, 164.

[35]. Castiglioni C., Gussoni M., Lopez-Navarrete J.T., Zerbi G., Solid State Comm. **1988**, *65*, 625.

[36]. Castiglioni C., Tommasini M., Zerbi G., Phil. Trans. R. Soc. Lond. A **2004**, *362*, 2425.

[37]. Ehrenfreund E., Vardeny Z., Brafman O., Horovitz B., Phys. Rev. B **1987**, *36*, 1535.

[38]. Milani A., Lucotti A., Russo V., Tommasini M., Cataldo F., Li Bassi A., and Casari C. S. J. Phys. Chem. C **2011**, *115*, 12836–12843.

[39]. Innocenti, F.; Milani, A.; Castiglioni, C. J. Raman Spectrosc. **2010**, *41*, 226.

[40]. Yang S., Kertesz M., Zolyomi V., Kürti J., J. Phys. Chem. A **2007**, *111*, 2434.

[41]. Yang S., Kertesz M., J. Phys. Chem. A **2008**, *112*, 146.

[42]. Januszewski J. A., Wendinger D., Methfessel C. D., Hampel F.and Tykwinski R. R., Angew. Chem., Int. Ed., **2013**, *52*, 1817–1821.

[43]. Januszewski J.A. and Tykwinski R.R. Chem. Soc. Rev., **2014**,*43*, 3184-3203.

[44]. Ravagnan L., Piseri P., Bruzzi M., Miglio S., Bongiorno G., Baserga A., Casari C.S., Li Bassi A., Lenardi C., Yamaguchi Y., Wakabayashi T., Bottani C.E., Milani P. Physical Review Letters **2007**, *98*, 216103.

[45]. Bogana M., Ravagnan L., Casari C.S., Zivelonghi A., Baserga A., Li Bassi A., Bottani C.E., Vinati S., Salis E., Piseri P., Barborini E., Colombo L., Milani P. New Journal of Physics **2005**, *7*, 81 1-8.

[46]. Casari C.S., Li Bassi A., Ravagnan L., Siviero F., Lenardi C., Piseri P., Bongiorno G., Bottani C.E., Milani P., Physical Review B, **2004**, *69*, 075422.

[47]. D'Urso L., Compagnini G., Puglisi O. et al. Journal of Physical Chemistry C **2007**, *111*, 17437.

[48]. Compagnini G., Battiato S., Puglisi O., Scandurra A., and Cataliotti R.S. Carbon **2005**, *43*, 3025-3028.

[49]. Hu A., Rybachuk M., Lu Q.-B., and Duley W. W., Applied Physics Letters **2007**, *91*, 131906.

[50]. Hu A., Lu Q.-B., Duley W. W., Rybachuk M. J. Chem. Phys. **2007**, *126*, 154705.

[51]. Cataldo F. Carbon **2003**, *41*, 2671.

[52]. Cataldo F. Tetrahedron **2004**, *60*, 4265–4274.

[53]. Szafert S. and Gladysz J.A., Chemical Reviews **2003**, *103*, 4175-205.

[54]. Kano E., Takeguchia M., Fujitaa J., Hashimoto A., Carbon **2014,** 80, 382–386.

[55]. Troiani H.E. Miki-Yoshida M., Camacho-Bragado G. A., Marques M. A. L., Rubio A., Ascencio J. A., and Jose-Yacaman M., Nano Lett. **2003**, 3, 751.

[56]. Chuvilin A., Meyer J.C., Algara-Siller G. and Kaiser U., New J. Phys. **2009**, 11, 083019.

[57]. Cretu O., Botello-Mendez A.R., Janowska I., Pham-Huu C., Charlier J.-C., and Banhart F. Nano Lett. **2013**, 13, 3487.

[58]. Casillas G., Mayoral A., Liu M., Ponce A., Artyukhov V.I., Yakobson B.I., Jose-Yacaman.M., Carbon **2014**, 66, 436.]

[59]. Casari C.S., Russo V., Li Bassi A., Bottani C.E., Cataldo F., Lucotti A., Tommasini M., Del Zoppo M., Castiglioni C., Zerbi G. Applied Physics Letters **2007**, *90***,** 13111.

[60]. Okada S., Fujii M., Hayashi S. Carbon **2011**, *49*, 4704-4709.

[61]. Tabata H., Fujii M., Hayashi S., Doi T., Wakabayashi T., Carbon **2006**, *44*, 3168-3176.

[62]. Lucotti A., Tommasini M., Fazzi D., Del Zoppo M., Chalifoux W.A., Ferguson M.J., Zerbi G., and Tykwinski R.R. J. Am. Chem. Soc. **2009**, *131*, 4239-44.

[63]. Cataldo F. and Casari C.S., J. Inorg. Organ. Pol. and Mater. **2007**, *17*, 641-651.

[64]. Chalifoux W.A. and Tykwinski R.R., Nature Chemistry **2010**, *2*, 967-71.

[65]. Ravagnan L., Manini N., Cinquanta E., Onida G., Sangalli D.,Motta C., Devetta M., Bordoni A., Piseri P., and Milani P. Physical Review Letters **2009,** *102*, 245502.

[66]. Casari C.S., Li Bassi A., Baserga A., Ravagnan L., Piseri P., Lenardi C., Tommasini M., Milani A., Fazzi D., Bottani C.E., Milani P. Physical Review B **2008**, *77*, 195444.

[67]. Yildizhan M.M., Fazzi D., Milani A., Brambilla L., Del Zoppo M., Chalifoux W.A., Tykwinski R. R., and Zerbi G. Journal of Chemical Physics **2011**, *134*, 124512.

[68]. Cataldo F. J. of Inorg. and Organomet. Polym. and Mater. **2006**, *16*, 15.

[69]. Cadierno V. and Gimeno J., Chemical Reviews **2009**, *109*, 3512-60.

[70]. Lucotti A., Tommasini M., Fazzi D., Del Zoppo M., Chalifoux W.A., Tykwinski R.R., Zerbi G., Journal of Raman Spectroscopy, **2012**, *43*, 1293-1298.

[71]. Agarwal N.R., Lucott A. i, Fazzi D., Tommasini M., Castiglioni C., Chalifoux W.A., Tykwinsk R.R. i, J. Raman Spectr. **2013,** *44*, 1398–1410

[72]. V.I. Artyukhov, Liu M., and Yakobson B.I., Nano Lett. 14, 4224 (2014)

[73]. C. Castiglioni, A. Milani, D. Fazzi, F. Negri J. Mol. Struct. **2011**, *993*, 26.

[74]. M. Liu, Artyukhov V.I., Lee H., Xu F., and Yakobson B.I., ACS Nano 7, 10075 (2013)

[75]. Lucotti A., Tommasini M., Del Zoppo M., Castiglioni C., Zerbi G., Cataldo F., Casari C.S., Li Bassi A., Russo V., Bogana M., Bottani C.E., Chem. Phys. Lett. **2006**, *417*, 78.

[76]. Lucotti A., Tommasini M., Del Zoppo M., Castiglioni C., Zerbi G., Cataldo F., Casari C.S., Li Bassi A., Russo V., Bogana M., Bottani C.E., Chem. Phys. Lett. **2009**, *478*, 45–50.

[77]. Cataldo F., Ursini O., Angelini G., Tommasini M., Casari C.S. Journal of Macromolecular Science, Part A: Pure and Applied Chemistry **2010**, *47*, 1–8.

[78]. Weimer M., Hieringer W., Della Sala F., Goerling A. Chemical Physics **2005**, *309*, 77–87.

[79]. Zanolli Z., Onida G., Charlier J-C, ACS Nano **2010**, *4*, 5174-80.

[80]. Wang C., Batsanov A.S., Bryce M.R., Martın S., Nichols R.J., Higgins S.J., Garcia-Suarez V. M., and Lambert C.J., J. Am. Chem. Soc. **2009**, *131*, 15647-54.

[81]. Moreno-Garcia P., Gulcur M., Manrique D. Z., Pope T., Hong W., Kaliginedi V., Huang C., Batsanov A.S., Bryce M.R., Lambert C. and Wandlowski T., J. Am. Chem. Soc. **2013**, *135*, 12228.

[82]. Standley B., Bao W., Zhang H., Bruck J., Lau C.N., and Bockrath M. Nano Letters **2008**, *8*, 3345

[83]. Yuzvinsky T. D., Mickelson W., Aloni S., Begtrup G. E., Kis A., and Zettl A. Nano Letters **2006**, *6,* 2718.

[84]. F. Diederich, and M. Kivala, Adv. Mater. **2010**, *22*, 803–812.

[85]. Malko D., Neiss C., Vines F., and Goerling A., PRL **2012**, *108*, 086804.